Supporting Information for

Trends in South Pole Particle Concentrations Imply Holocene Westerly Wind Strengthening

A. Chesler[1,2],*, D. Winski[1,2], K.J. Kreutz[1,2], B.G. Koffman[3], E.C. Osterberg[4], D. Ferris[4], Z. Thundercloud[4], J. Cole-Dai[5], M. Wells[6], A.E. Putnam[1,2], and K. Anderson[4]

1Climate Change Institute, University of Maine, Orono, Maine, 04469, USA

2 School of Earth and Climate Sciences, University of Maine, Orono, Maine, 04469, USA

3Department of Geology, Colby College, Waterville, Maine, 04901, USA

4Department of Earth Sciences, Dartmouth College, Hanover, New Hampshire, 03755, USA

5Department of Chemistry and Biochemistry, South Dakota State University, Brookings, South Dakota, 57007, USA

6School of Marine Sciences, University of Maine, Orono, Maine, 04469, USA

Corresponding author: Aaron Chesler (achesler2023@coloradocollege.edu)

*now at: Environmental Studies and Science Department, Colorado College, Colorado Springs, Colorado, 80903, USA

Contents of this file

Text S1. Additional Methods

We use a subset of the total Abakus size bins (21 of 30 size bins) ranged continuously in 0.1μm increments from endpoints (lower) 1.0 – 2.5 μm, followed by bins

2.7, 2.9, 3.2, 3.6, 4.0, and 4.5 µm, with and upper limit of 5.1µm. We use this subset to match other dust concentration methodology from East Antarctica (i.e., Delmonte et al., 2020). The CFA system has an effective resolution of 3 mm with a dispersion signal of 1 cm (Breton et al., 2012; Osterberg et al., 2006; Winski et al., 2019). The SPC14 chronology within the top 5 – 796 m (< 11,300 years BP) is annually resolved and was developed using seasonal variations in Na^{+} and Mg^{2+} ions constrained by volcanic tie points (Winski et al., 2019). Age uncertainty during the Holocene is <18 years except between 3100 – 1800 years BP where the uncertainty increases to ~25 years relative to the WD2014 timescale (Buizert et al., 2015; Sigl et al., 2016; Winski et al., 2019). To mitigate contamination from fractured sections of core that contain trace amounts of Estisol-140 and other impurities (Warming et al., 2013), we used a Python-based cleaning code (Chesler et al., 2023) to detect and remove inferred Estisol-140-related peaks in the Abakus data. While overlapping Abakus dust measurements (i.e., coincidence) can influence dust measurement counts, prior work (Chesler et al., 2023) found no significant evidence of coincidence in the SPC14 dust record.

We use a spherical particle shape assumption to facilitate comparison to other Antarctica ice core particle records that include a volume assumption (i.e., flux). While this produces higher-than-realistic particle flux values, it mitigates discrepancies from comparing dissimilar metrics, whereas in the past particle shape has been assumed to be spherical (Chesler et al., 2023; Potenza et al., 2016; Simonsen et al., 2018). Studies concerned with the absolute magnitude of dust flux at the South Pole should use prolate particle shapes to calculate flux (Chesler et al., 2023; data at USAP-DC, DOI: 10.15784/601553).

Text S2. CPP sources and ^{10}Be calibration

Course particle percentage (CPP) is hypothesized to reflect local Antarctic dust source activity, where increases in CPP reflect activation of local dust sources and a decrease reflects either a more active distal mid-latitudinal source or a decrease in local sources (Aarons et al., 2016; Albani et al., 2012; Koffman et al., 2014). We therefore compare the timing of CPP increase to coastal Antarctic glacier surface elevation lowering, to assess activation of local Antarctic dust sources. Because published surface exposure ages (^{10}Be) were calculated using different calibration rates, we recalibrate ^{10}Be surface exposure ages from the Pine Island Glacier (Johnson et al., 2014), Ross Sea (Jones et al., 2015; Jones et al., 2020), and Dronning Maud Land (Kawamata et al., 2020) using the University of Washington exposure age calculator, using production rates from Putnam et al. (2010) and Kaplan et al. (2011), and using the Lm scaling factor (Balco et al., 2008).

Text S3. Atmospheric Distillation

Changes in aerosol particle concentration may also be induced by atmospheric distillation, which results from variability in temperature and humidity gradients (Markle et al., 2018). If this mechanism were primarily responsible for the decrease in Holocene dust, we would expect associated changes in temperature and/or stable water isotopes, as is the case on glacial/interglacial timescales (Markle et al., 2018). However, Antarctic paleoproxy records indicate only modest Holocene temperature changes and there is no significant relationship between dust concentration and SPC14 δ^{18}O (Kahle et al., 2020; Steig et al., 2021). Therefore, atmospheric distillation processes were likely not a major driver of altering the transport of dust to the South Pole during the Holocene.

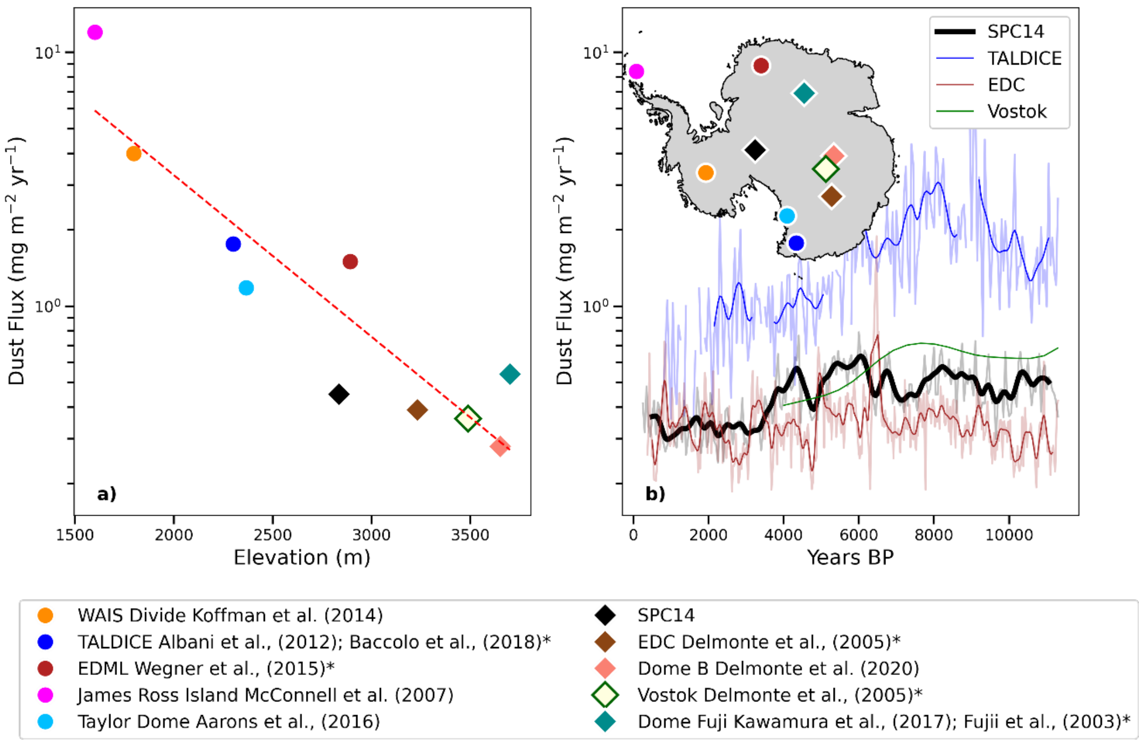

Figure S1a and b: Comparison of SPC14 dust metrics with other Antarctic Holocene records. Plateau sites are depicted with diamonds while non-plateau (i.e., WAIS and coastal locations) are depicted with circles. Labels containing a * symbol at the end were reported in (Delmonte et al., 2020). In S1a, SPC14 dust flux is similar to other cores based on drill site elevation. S1b shows available Holocene flux records from Talos Dome fine particle flux (0.6 – 5 µm mg m^{-2} yr^{-1}) (Albani et al., 2012), Vostok (Petit et al., 1990), EPICA Dome C (EDC; Lambert et al., 2012). SPC14 dust flux is similar to other East Antarctic sites (Vostok and EDC) and is on average ~67% lower compared to TALDICE. TALDICE, SPC14, and EDC were resampled to 50-year median values (background variability), and the darkened lines are the 11-point rolling gaussian mean for TALDICE, SPC14, and EDC.

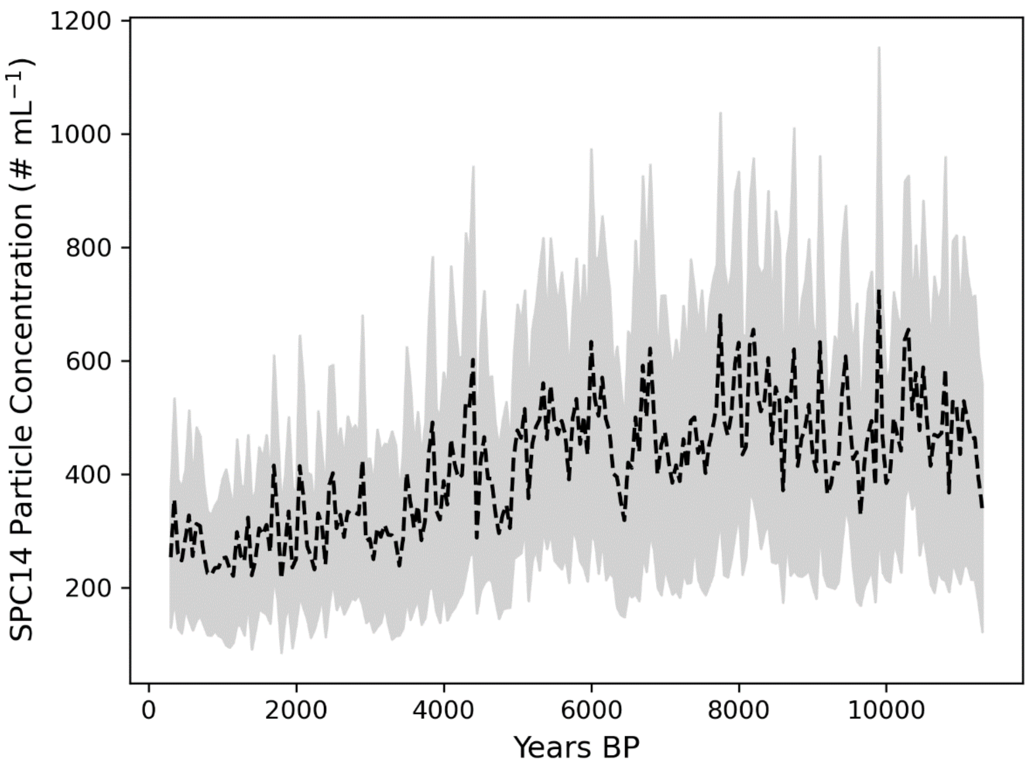

Figure S2: Median SPC14 Particle concentration in black dashed line with concentrations within median absolute deviation (MAD) shaded in the light grey.

Table S1: Median dust metrics and standard deviations for different time periods (2σ).

	Dust Concentration (# mL^{-1})	CPP (%)	Dust Flux (mg m^{-2} yr^{-1})
Average Holocene	418 ± 244	8.9 ± 1.3	0.43 ± 0.22
Early Holocene (11,300 – 7,000 years BP)	471 ± 166	8.6 ± 2.8	0.45 ± 0.17
Mid Holocene (7,000 – 3,000 years BP)	421 ± 190	8.9 ± 1.1	0.46 ± 0.22
Late Holocene (3000 – 250 years BP)	286 ± 108	9.4 ± 1.1	0.32 ± 0.11

Table S2a and b. Student t-test comparison of a) particle concentration and b) CPP distributions between the early, mid-, and late Holocene.

2a)

	Late Holocene	Middle Holocene	Early Holocene
Late Holocene	X	t-statistic = -8.4 p-value = <0.01	t-statistic = -14.6 p-value = <0.01
Middle Holocene	X	X	t-statistic = -4.9 p-value = <0.01
Early Holocene	X	X	X

2b)

	Late Holocene	Middle Holocene	Early Holocene
Late Holocene	X	t-statistic = 3.9 p-value = <0.01	t-statistic = 5.4 p-value = <0.01
Middle Holocene	X	X	t-statistic = 2.2 p-value = >0.01
Early Holocene	X	X	X

References From the Supporting Information.

Aarons, S. M., Aciego, S. M., Gabrielli, P., Delmonte, B., Koornneef, J. M., Wegner, A., & Blakowski, M. A. (2016). The impact of glacier retreat from the Ross Sea on local climate: Characterization of mineral dust in the Taylor Dome ice core, East Antarctica. *Earth and planetary science letters, 444*, 34-44. doi:10.1016/j.epsl.2016.03.035

Albani, S., Delmonte, B., Maggi, V., Baroni, C., Petit, J. R., Stenni, B., . . . Frezzotti, M. (2012). Interpreting last glacial to Holocene dust changes at Talos Dome (East Antarctica): implications for atmospheric variations from regional to hemispheric scales. *Climate of the past, 8*(2), 741-750. doi:10.5194/cp-8-741-2012

Balco, G., Stone, J. O., Lifton, N. A., & Dunai, T. J. (2008). A complete and easily accessible means of calculating surface exposure ages or erosion rates from ^{10}Be and ^{26}Al measurements. *Quaternary Geochronology, 3*(3), 174-195. doi:10.1016/j.quageo.2007.12.001

Breton, D. J., Koffman, B. G., Kurbatov, A. V., Kreutz, K. J., & Hamilton, G. S. (2012). Quantifying Signal Dispersion in a Hybrid Ice Core Melting System. *Environmental Science & Technology, 46*(21), 11922-11928. doi:10.1021/es302041k

Buizert, C., Cuffey, K. M., Severinghaus, J. P., Baggenstos, D., Fudge, T. J., Steig, E. J., . . . Taylor, K. C. (2015). The WAIS Divide deep ice core WD2014 chronology – Part 1: Methane synchronization (68–31 ka BP) and the gas age–ice age difference. *Clim. Past, 11*(2), 153-173. doi:10.5194/cp-11-153-2015

Chesler, A., Winski, D., Kreutz, K., Koffman, B., Osterberg, E., Ferris, D., . . . Harmon, N. (2023). Non-spherical microparticle shape in Antarctica during the last glacial period affects dust volume-related metrics. *Clim. Past, 19*(2), 477-492. doi:10.5194/cp-19-477-2023

Delmonte, B., Winton, H., Baroni, M., Baccolo, G., Hansson, M., Andersson, P., . . . Maggi, V. (2020). Holocene dust in East Antarctica: Provenance and variability in time and space. *The Holocene, 30*(4), 546-558. doi:10.1177/0959683619875188

Johnson, J. S., Bentley, M. J., Smith, J. A., Finkel, R. C., Rood, D. H., Gohl, K., . . . Schaefer, J. M. (2014). Rapid Thinning of Pine Island Glacier in the Early Holocene. *Science, 343*(6174), 999-1001. doi:doi:10.1126/science.1247385

Jones, R. S., Mackintosh, A. N., Norton, K. P., Golledge, N. R., Fogwill, C. J., Kubik, P. W., . . . Greenwood, S. L. (2015). Rapid Holocene thinning of an East Antarctic outlet glacier driven by marine ice sheet instability. *Nature communications, 6*(1), 8910. doi:10.1038/ncomms9910

Jones, R. S., Whitmore, R. J., Mackintosh, A. N., Norton, K. P., Eaves, S. R., Stutz, J., & Christl, M. (2020). Regional-scale abrupt Mid-Holocene ice sheet thinning in the western Ross Sea, Antarctica. *Geology, 49*(3), 278-282. doi:10.1130/g48347.1

Kahle, E., Buizert, C., Conway, H., Epifanio, J., Fudge, T. J., & Jones, T. R. (2020). *Temperature, accumulation rate, and layer thinning from the South Pole ice core (SPC14)*.

Kaplan, M. R., Strelin, J. A., Schaefer, J. M., Denton, G. H., Finkel, R. C., Schwartz, R., . . . Travis, S. G. (2011). In-situ cosmogenic 10Be production rate at Lago Argentino, Patagonia: Implications for late-glacial climate chronology. *Earth and planetary science letters, 309*(1), 21-32. doi:10.1016/j.epsl.2011.06.018

Kawamata, M., Suganuma, Y., Doi, K., Misawa, K., Hirabayashi, M., Hattori, A., & Sawagaki, T. (2020). Abrupt Holocene ice-sheet thinning along the southern Soya Coast, Lützow-Holm Bay, East Antarctica, revealed by glacial geomorphology and surface exposure dating. *Quaternary science reviews, 247*, 106540. doi:10.1016/j.quascirev.2020.106540

Koffman, B. G., Kreutz, K. J., Breton, D. J., Kane, E. J., & Winski, D. A. (2014). Centennial-scale variability of the Southern Hemisphere westerly wind belt in the eastern Pacific over the past two millennia. *Climate of the past, 10*(3), 1125-1144. doi:10.5194/cp-10-1125-2014

Lambert, F., Bigler, M., Steffensen, J. P., Hutterli, M., & Fischer, H. (2012). Centennial mineral dust variability in high-resolution ice core data from Dome C, Antarctica. *Clim. Past, 8*(2), 609-623. doi:10.5194/cp-8-609-2012

Markle, B. R., Steig, E. J., Roe, G. H., Winckler, G., & McConnell, J. R. (2018). Concomitant variability in high-latitude aerosols, water isotopes and the hydrologic cycle. *Nature geoscience, 11*(11), 853-859. doi:10.1038/s41561-018-0210-9

Osterberg, E. C., Handley, M. J., Sneed, S. B., Mayewski, P. A., & Kreutz, K. J. (2006). Continuous ice core melter system with discrete sampling for major ion, trace element, and stable isotope analyses. *Environmental Science & Technology, 40*(10), 3355-3361. doi:10.1021/es052536w

Petit, J. R., Mourner, L., Jouzel, J., Korotkevich, Y. S., Kotlyakov, V. I., & Lorius, C. (1990). Palaeoclimatological and chronological implications of the Vostok core dust record. *Nature, 343*(6253), 56-58.

Potenza, M. A. C., Albani, S., Delmonte, B., Villa, S., Sanvito, T., Paroli, B., . . . Maggi, V. (2016). Shape and size constraints on dust optical properties from the Dome C ice core, Antarctica. *Scientific reports, 6*, 9. doi:10.1038/srep28162

Putnam, A. E., Schaefer, J. M., Barrell, D. J. A., Vandergoes, M., Denton, G. H., Kaplan, M. R., . . . Kelley, S. E. (2010). In situ cosmogenic ^{10}Be production-rate calibration from the Southern Alps, New Zealand. *Quaternary Geochronology, 5*(4), 392-409. doi:10.1016/j.quageo.2009.12.001

Sigl, M., Fudge, T. J., Winstrup, M., Cole-Dai, J., & Ferris, D. (2016). The WAIS Divide deep ice core WD2014 chronology – Part 2: Annual-layer counting (0–31 ka BP). *Climate of the past, 12*(3), 769-786. doi:10.5194/cp-12-769-2016

Simonsen, M. F., Cremonesi, L., Baccolo, G., Bosch, S., Delmonte, B., Erhardt, T., . . . Vallelonga, P. (2018). Particle shape accounts for instrumental discrepancy in ice core dust size distributions. *Clim. Past Discuss.*, 19 (in press).

Steig, E. J., Jones, T. R., Schauer, A. J., Kahle, E. C., Morris, V. A., Vaughn, B. H., . . . White, J. W. C. (2021). Continuous-Flow Analysis of δ17O, δ18O, and δD of H2O on an Ice Core from the South Pole. *Frontiers in Earth Science, 9*. doi:10.3389/feart.2021.640292

Warming, E., Svensson, A., Vallelonga, P., & Bigler, M. (2013). A technique for continuous detection of drill liquid in ice cores. *Journal of Glaciology, 59*(215), 503-506. doi:10.3189/2013JoG12J124

Winski, D. A., Fudge, T. J., Ferris, D. G., Osterberg, E. C., Fegyveresi, J. M., Cole-Dai, J., . . . McConnell, J. R. (2019). The SP19 chronology for the South Pole Ice Core – Part 1: volcanic matching and annual layer counting. *Clim. Past, 15*(5), 1793-1808. doi:10.5194/cp-15-1793-2019